



OPEN

Development of deep learning chest X-ray model for cardiac dose prediction in left-sided breast cancer radiotherapy

Yutaro Koide[✉], Takahiro Aoyama, Hidetoshi Shimizu, Tomoki Kitagawa, Risei Miyauchi, Hiroyuki Tachibana & Takeshi Kodaira

Deep inspiration breath-hold (DIBH) is widely used to reduce the cardiac dose in left-sided breast cancer radiotherapy. This study aimed to develop a deep learning chest X-ray model for cardiac dose prediction to select patients with a potentially high risk of cardiac irradiation and need for DIBH radiotherapy. We used 103 pairs of anteroposterior and lateral chest X-ray data of left-sided breast cancer patients (training cohort: $n = 59$, validation cohort: $n = 19$, test cohort: $n = 25$). All patients underwent breast-conserving surgery followed by DIBH radiotherapy: the treatment plan consisted of three-dimensional, two opposing tangential radiation fields. The prescription dose of the planning target volume was 42.56 Gy in 16 fractions. A convolutional neural network-based regression model was developed to predict the mean heart dose (Δ MHD) reduction between free-breathing (MHD_{FB}) and DIBH. The model performance is evaluated as a binary classifier by setting the cutoff value of Δ MHD > 1 Gy. The patient characteristics were as follows: the median (IQR) age was 52 (47–61) years, MHD_{FB} was 1.75 (1.14–2.47) Gy, and Δ MHD was 1.00 (0.52–1.64) Gy. The classification performance of the developed model showed a sensitivity of 85.7%, specificity of 90.9%, a positive predictive value of 92.3%, a negative predictive value of 83.3%, and a diagnostic accuracy of 88.0%. The AUC value of the ROC curve was 0.864. The proposed model could predict Δ MHD in breast radiotherapy, suggesting the potential of a classifier in which patients are more desirable for DIBH.

Abbreviations

DIBH	Deep inspiration breath-hold
MHD	Mean heart dose
FB	Free-breathing
RT	Radiotherapy
BMI	Body mass index
MHD_{FB}	MHD in FB
MHD_{DIBH}	MHD in DIBH
ML	Machine learning
CTV	Clinical target volume
PTV	Planning target volume
MLC	Multileaf collimator
CNN	Convolutional neural network
ReLU	Rectified linear units
R^2	Coefficient of determination
RMSE	Root mean squared error
MAE	Mean absolute error

Late cardiac toxicity after breast irradiation is a major adverse event in left-sided breast radiotherapy (RT)^{1–6}. Darby et al. showed the relationship between the mean heart dose (MHD) and the frequency of major coronary events⁵. Deep inspiration breath-hold (DIBH) effectively reduces MHD compared to free-breathing (FB) RT^{7–12}.

Department of Radiation Oncology, Aichi Cancer Center, Kanokoden 1-1, Chikusa-ku, Nagoya, Aichi, Japan. ✉email: ykoide@aichi-cc.jp

Rochet et al. reported in their study that the reduction of MHD was > 0.9 Gy in 75% of patients and < 0.9 Gy in 25%¹³. Past studies have attempted to predict MHD using some parameters acquired in the simulation CT^{14–27}. Most studies used such CT-based parameters, but some used non-CT parameters (e.g., BMI, pulmonary function test)^{14,28–34}. Although non-CT parameters may have advantages over CT parameters in terms of earlier availability and reduced patient radiation exposure, no reports have high prediction accuracy using non-CT parameters. We previously investigated non-radiological parameters for preoperative prediction of MHD. Vital capacity was a significant predictor of MHD in DIBH (MHD_{DIBH}), but it still did not work as an accurate prediction³⁴.

The machine learning (ML) technique has been widely used in the medical field^{35,36}. Many studies have used the ML approach with radiological images, and recently chest X-rays have been actively studied as a diagnostic ML tool in Covid-19^{37,38}. Chest X-rays are the most frequently taken and easily available radiological images. Therefore, we wondered if the ML chest X-ray model could predict the cardiac dose of the breast RT, it might be easier and earlier to select which patients have significant benefit from DIBH.

The purpose of this study is to predict MHD in FB (MHD_{FB}) and MHD reduction between DIBH and FB (Δ MHD) using a machine learning method with preoperative chest X-rays.

Methods

Patient selection. This study is a prediction model development study approved by our institutional review board. All participants provided written informed consent and all methods were performed in accordance with the relevant guidelines and regulations. The eligibility criteria are as follows: histologically proven diagnosis of invasive ductal carcinoma or carcinoma in situ of the left breast, patients who underwent DIBH-RT after breast-conserving surgery from June 2018 to October 2021. Patients who did not receive preoperative chest X-rays were excluded. All data were retrospectively collected randomly split into two cohorts (training cohort: $n = 78$, test cohort: $n = 25$).

Planning CT simulation. The DIBH-RT method of this study has implemented a technique of Bartlett et al.¹⁰. Described as our previous study, we trained patients to inhale, exhale, and hold deep breaths. The breath-hold training time was initially 5–10 s and increased to 20 s^{26,34}. The simulation and training took about 20–30 min per patient. After confirming the respiratory motion, all patients underwent two planning CT simulations (FB and DIBH) in the supine position on a wing board with the arms stretched overhead. We used the Aquilion LB CT system (Canon Medical Systems, Tochigi, Japan) with a slice thickness of 3 mm.

Treatment planning. We perform the contouring and planning on FB- and DIBH-CT using RayStation version 9 (RaySearch Laboratories AB, Stockholm, Sweden). The calculation algorithm is Collapsed Cone version 5.1. The planning target volume (PTV), including CTV with a 5-mm margin, was prescribed 42.56 Gy in 16 fractions with the Varian TrueBeam system (Varian Medical Systems, Palo Alto, USA)^{26,34}. The clinical target volume (CTV) and the heart were delineated following the consensus guideline and atlas validation study^{39,40}. The CTV was cropped withing 5 mm of the skin contour. Treatment plans consist of three-dimensional conformal radiotherapy using two opposing tangential beams and a field-in-field technique.

Development of the chest X-ray model. Figure 1 shows a pipeline outlining the modeling procedure and evaluation.

As the Transparent Reporting of a multivariable prediction model for Individual Prognosis Or Diagnosis (TRIPOD) guideline described, the data is split into the following groups; Model development group (Training: $N = 59$, Validation: $N = 19$), and Test group (Test: $N = 25$)⁴¹. Although the optimal ratio for the number of patients in each group has not been established, 60/20/20 and 70/15/15 are frequently used empirically; The ratio of each group in this study was determined based on several previous studies^{27,42}. A regression model was trained with the training group, and the predicted MHD was validated against the validation group. Input values and size were searched from the parameters in previous studies and finally determined to achieve the best prediction results in the validation group^{26,27,30,34,42}. Table 1 shows the convolutional neural network (CNN) architecture with the determined parameters.

The architecture has three inputs: an anteroposterior chest X-ray image (1, 64, 64) as input 1, a lateral chest X-ray image (1, 64, 64) as input 2, and a patient's age (y), height (cm), and weight (kg) as input 3. First, we multiply the input1 and two tensors at the element level (i.e., multiplying each pixel of images). Then, convolution is performed twice for the multiplied data (1, 64, 64), followed by Rectified Linear Units (ReLU) and batch normalization. The resulting tensors were then fully connected and concatenated with input 3. Then performed another full-connection process, The predicted MHD was produced as an absolute value of the final output. Finally, predicted MHD is trained using the mean squared error as the loss function with 100 epochs.

Model evaluation and statistical analyses. The primary prediction outcome is Δ MHD. The model is trained to achieve a high prediction accuracy of Δ MHD in the training cohort. The prediction performance of the developed model is evaluated in an independent test cohort. As our previous study²⁶, we use the model as a binary classifier to determine if a patient would potentially receive Δ MHD > 1 Gy or not. The model performance is also evaluated as a regression model by calculating the median and interquartile range of absolute residuals, the coefficient of determination (R^2), root mean squared error (RMSE), and mean absolute error (MAE). The secondary outcome is defined as the prediction accuracy of MHD_{FB}. The prediction performance is evaluated in the same way as the primary outcome, but the cutoff value of classification is set as MHD_{FB} > 2 Gy following some previous reports^{6,43,44}.

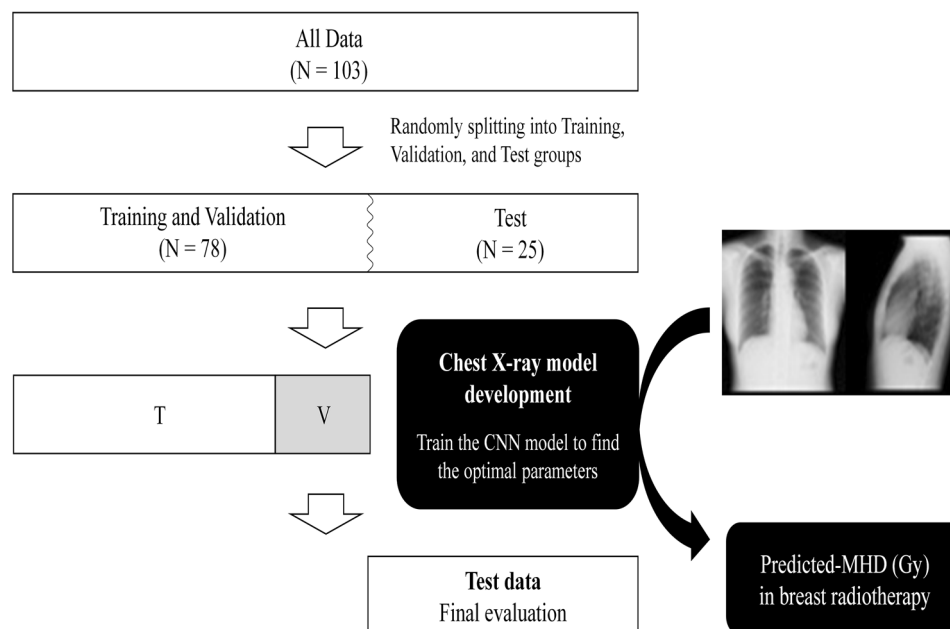


Figure 1. A pipeline of modeling procedure and model evaluation. *T* training, *V* validation, *CNN* convolutional neural network, *MHD* mean heart dose.

Layer	Output Shape	Connected to
Input1: X1 Input2: X2	1, 64, 64 1, 64, 64	
Mul ($X2 \times X1$)	1, 64, 64	Input1, 2
Conv_1 Batch_norm_1 ReLU_1	16, 30, 30	Mul ($X2 \times X1$)
Conv_2 Batch_norm_2 ReLU_2	16, 30, 30	ReLU_1
Dropout	16, 30, 30	ReLU_2
Full_connection_1 Batch_norm_3	100	Dropout
Full_connection_2	100	Batch_norm_3
Concatenate	103	Input3: X3 Full_connection_2
Full_connection_3 ReLU_3	100	Concatenate
Full_connection_4	1	ReLU_3

Table 1. The detailed structure of CNN used in this study. *CNN* convolutional neural network, *Mul* multiply, *Conv* convolution, *Batch_norm* batch normalization, *ReLU* rectified linear unit.

Statistical analysis was performed using R version 3.6.1 (The R Foundation for Statistical Computing, Vienna, Austria). The required sample size of test data is based on Δ MHD: we set the cutoff value of <1 Gy as the classification point. According to our training data, 50% of patients had >1 Gy. We estimated at least ten events (i.e., 20 patients) are required. $P < 0.05$ (two-sided) was considered statistically significant.

Ethics approval and consent to participate. The Institutional Review Board (IRB) of Aichi Cancer Center Hospital approved our study (approve number: 2019-1-211).

Results

Dataset. One hundred and three patients were included in this study. Table 2 shows the patient characteristics of the training and test cohort. Each characteristic difference was not statistically significant between the cohorts. In the test cohort, median Δ MHD and MHD_{FB} were 1.24 (range 0.080–2.71) Gy and 1.97 (range 0.52–3.80) Gy, respectively. Fourteen patients (56%) had Δ MHD ≥ 1 Gy.

Characteristic	Training cohort (N = 78)	Test cohort (N = 25)
Age: median (IQR), years	52 (47–58)	58 (46–63)
Height: median (IQR), m	1.57 (1.54–1.60)	1.55 (1.52–1.61)
Weight: median (IQR), kg	54.0 (47.5–62.0)	51.3 (46.1–58.3)
The interval between chest X-ray and radiotherapy, median (IQR), days	82 (66–102)	104 (77–133)
Tumor site		
Inner-upper (A)	16	4
Inner-lower (B)	6	3
Outer-upper (C)	43	15
Outer-lower (D)	13	3
Center (E)	2	0
TNM		
Tis	12	2
T1N0	49	17
T2N0	10	3
T1–2N1	7	2
Other	0	1
Molecular subtypes		
Luminal (HR-positive and HER2 negative)	56	15
HER2 (HR negative and HER2 positive)	8	3
Luminal HER2 (HR and HER2 positive)	6	3
Triple-negative (HR and HER2 negative)	6	3
Unknown or other	2	1
Neoadjuvant chemotherapy, Y/N	13/65	6/19
Surgery		
BCS alone	2	2
BCS + SLNB (No ALND)	70	20
BCS + ALND	4	1
Other	2	2
Adjuvant chemotherapy, Y/N	7/71	3/22

Table 2. Patient characteristics. *BCS* breast-conserving surgery, *SLNB* sentinel lymph node biopsy, *ALND* axillary lymph node dissection, *IQR* interquartile range.

Model performance: MHD prediction results. As a binary classifier of $\Delta\text{MHD} > 1$ Gy, the model showed a high classification performance: a sensitivity of 85.7%, a specificity of 90.9%, a positive predictive value of 92.3%, a negative predictive value of 83.3%, and diagnostic accuracy of 88.0%. Figure 2 shows the ROC curve, and the AUC value is 0.864 (95% CI 0.701–1.00). The point at 1.02 Gy was the best classification point in which the sum values of the sensitivity and specificity were maximized.

The developed model shows that the median predicted ΔMHD was 1.02 (range 0.06–2.43, IQR 0.63–2.11) Gy. Compared to the observed ΔMHD , the absolute prediction difference was 0.39 (range 0.004–1.55, IQR: 0.22–0.72) Gy. The Pearson correlation coefficient between observed and predicted ΔMHD was 0.55 ($P = 0.028$). R^2 , RMSE, and MAE were 0.30, 0.73, 0.56, respectively.

Although the accuracy was not as ΔMHD , MHD_{FB} could also be predicted from the model: the median absolute error was 0.72 Gy (range 0.058–2.73 Gy, IQR 0.43–1.42 Gy), the correlation coefficient was 0.46 ($P = 0.02$), and the sensitivity and specificity were 0.58 and 0.77, respectively.

Discussion

Recent studies have attempted to predict MHD to select patients with potential cardiac toxicity risks and reduce MHD by performing DIBH^{14-26} . In most cases, prediction models used the maximum heart distance or cardiac contact distance in the CT simulations as predictors^{14-20,24}. The coronary artery calcium scores (CAC) in CT improved the Framingham risk score prediction for coronary artery disease (CAD)^{45,46}. According to Mast et al., DIBH increases LAD CAC less than FB, potentially preventing radiation-induced coronary artery disease⁴⁷. Our previous study demonstrated that a synthetic DIBH-CT model with a deep learning approach achieved more accurate ΔMHD prediction than other models²⁶. However, such models in past studies have a significant limitation: the prediction is only performed after simulation CT.

We next investigated non-radiological parameters for preoperative prediction of MHD^{34} . The result showed that Vital capacity was the only significant predictor of MHD_{DIBH} , but it could not work as a predictor of ΔMHD nor MHD_{FB} as other parameters. To the best of our knowledge, no other studies have found non-CT parameters promising as predictors of ΔMHD nor MHD_{FB} . Therefore, this study attempted to predict ΔMHD nor MHD_{FB} using a deep learning technique based on preoperative chest X-rays. The prediction results showed a high

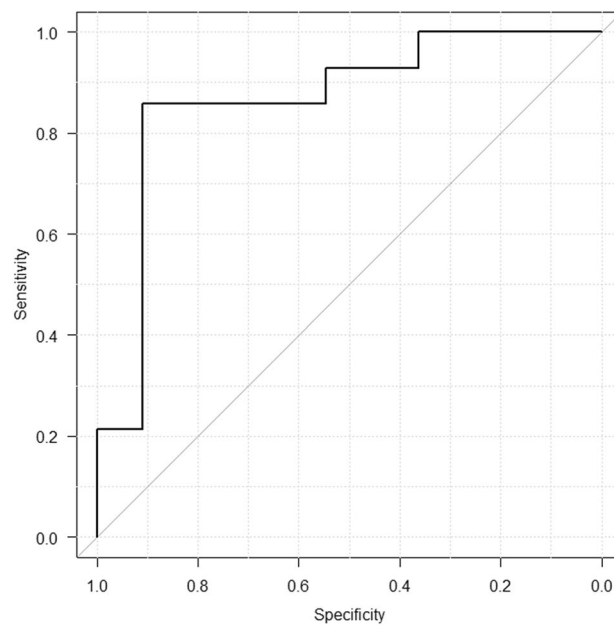


Figure 2. The Receiver Operating Characteristic (ROC) curve of the developed model: the area under curve (AUC) value was 0.864. The sensitivity and specificity of the best classification point (= 1.02 Gy) were 0.857 and 0.909, respectively.

performance as a binary classifier in the cutoff of $\Delta\text{MHD} > 1$ Gy. Our model has also worked for MHD_{FB} prediction in the same method. The strong points of this model are the early timing of the prediction and the required radiological images required only chest X-rays, which can be acquired easier and earlier than simulation CT in many patients. Ninety-two percent of our patients underwent preoperative chest X-rays, with a median of 90 days before radiotherapy.

In the present study, MHD_{FB} and ΔMHD were used as predictive outcomes, following previous studies^{14,26,28–34}. The primary outcome was defined as ΔMHD , used in multiple studies^{14,26,30–33}. We set the cutoff for classification as $\Delta\text{MHD} > 1$ Gy based on the report of increased cardiotoxicity per 1 Gy by Darby et al.: a linear relationship between MHD and the frequency of major coronary events that increases at a rate of 7.4% per Gy, but no significant difference was found for $\text{MHD} < 2$ Gy⁵. Otherwise, the Early Breast Cancer Trialists' Collaborative Group report and the UK consensus statements for postoperative breast radiotherapy recommend the $\text{MHD} < 2$ Gy, so it may be possible to set the classification criteria with MHD_{FB} as the primary predictive outcome^{6,43,44}.

There are several limitations of this study. First, our study used a single institutional dataset, consisting mainly of those who underwent BCS followed by DIBH-RT. Therefore, whether the study results can be extrapolated to patients undergoing chest wall or lymph node irradiation is uncertain. Second, our approach focused on the chest X-ray parameters and may omit the clinical aspects of DIBH training during simulation: even if the prediction recommends the cardiac sparing RT, our model does not predict whether the patient can tolerate DIBH. Finally, the CNN architecture used in this study requires both anteroposterior and lateral chest X-ray images. Future studies are needed to build a model using only anteroposterior images and perform external validation at multicenter for model versatility.

Conclusion

In conclusion, our deep learning chest X-ray model can predict MHD and play an essential role in classifying patients' potentially desirable DIBH. However, further study is needed to validate our prediction model externally.

Data availability

Research data are stored in an institutional repository and anonymized numerical data will be shared upon request to the corresponding author. Research image data are not available at this time.

Received: 14 March 2022; Accepted: 12 July 2022

Published online: 12 August 2022

References

1. Correa, C. R. *et al.* Coronary artery findings after left-sided compared with right-sided radiation treatment for early-stage breast cancer. *J. Clin. Oncol.* **25**, 3031–3037 (2007).
2. Bouchardy, C. *et al.* Excess of cardiovascular mortality among node-negative breast cancer patients irradiated for inner-quadrant tumors. *Ann. Oncol.* **21**, 459–465 (2009).
3. Harris, E. E. R. *et al.* Late cardiac mortality and morbidity in early-stage breast cancer patients after breast-conservation treatment. *J. Clin. Oncol.* **24**, 4100–4106 (2006).

4. Cheng, Y. *et al.* Long-term cardiovascular risk after radiotherapy in women with breast cancer. *J. Am. Heart Assoc.* **6**, e005633 (2017).
5. Darby, S. C. *et al.* Risk of ischemic heart disease in women after radiotherapy for breast cancer. *N. Engl. J. Med.* **368**, 987–998 (2013).
6. Taylor, C. *et al.* Estimating the risks of breast cancer radiotherapy: Evidence from modern radiation doses to the lungs and heart and from previous randomized trials. *J. Clin. Oncol.* **35**, 1641–1649 (2017).
7. Lu, H. M. *et al.* Reduction of cardiac volume in left-breast treatment fields by respiratory maneuvers: A CT study. *Int. J. Radiat. Oncol. Biol. Phys.* **47**, 895–904 (2000).
8. Pandeli, C., Smyth, L. M. L., David, S. & See, A. W. Dose reduction to organs at risk with deep-inspiration breath-hold during right breast radiotherapy: A treatment planning study. *Radiat. Oncol.* **14**, 223 (2019).
9. Korreman, S. S., Pedersen, A. N., Nøttrup, T. J., Specht, L. & Nyström, H. Breathing adapted radiotherapy for breast cancer: Comparison of free breathing gating with the breath-hold technique. *Radiother. Oncol.* **76**, 311–318 (2005).
10. Bartlett, F. R. *et al.* The UK HeartSpare study: Randomised evaluation of voluntary deep-inspiratory breath-hold in women undergoing breast radiotherapy. *Radiother. Oncol.* **108**, 242–247 (2013).
11. Lee, H. Y. *et al.* The deep inspiration breath hold technique using Abches reduces cardiac dose in patients undergoing left-sided breast irradiation. *Radiat. Oncol. J.* **31**, 239–246 (2013).
12. Latty, D., Stuart, K. E., Wang, W. & Ahern, V. Review of deep inspiration breath-hold techniques for the treatment of breast cancer. *J. Med. Radiat. Sci.* **62**, 74–81 (2015).
13. Rochet, N. *et al.* Deep inspiration breath-hold technique in left-sided breast cancer radiation therapy: Evaluating cardiac contact distance as a predictor of cardiac exposure for patient selection. *Pract. Radiat. Oncol.* **5**, e127–e134 (2015).
14. Cao, N. *et al.* Predictors of cardiac and lung dose sparing in DIBH for left breast treatment. *Phys. Med.* **67**, 27–33 (2019).
15. Wang, W. *et al.* Rapid automated treatment planning process to select breast cancer patients for active breathing control to achieve cardiac dose reduction. *Int. J. Radiat. Oncol. Biol. Phys.* **82**, 386–393 (2012).
16. Dell’Oro, M. *et al.* A retrospective dosimetric study of radiotherapy patients with left-sided breast cancer; patient selection criteria for deep inspiration breath hold technique. *Cancers* <https://doi.org/10.3390/cancers11020259> (2019).
17. Tanna, N. *et al.* Assessment of upfront selection criteria to prioritise patients for breath-hold left-sided breast radiotherapy. *Clin. Oncol.* **29**, 356–361 (2017).
18. Kong, F.-M. *et al.* The impact of central lung distance, maximal heart distance, and radiation technique on the volumetric dose of the lung and heart for intact breast radiation. *Int. J. Radiat. Oncol. Biol. Phys.* **54**, 963–971 (2002).
19. Mohamad, O. *et al.* Deep inspiration breathhold for left-sided breast cancer patients with unfavorable cardiac anatomy requiring internal mammary nodal irradiation. *Pract. Radiat. Oncol.* **7**, e361–e367 (2017).
20. Register, S. *et al.* Deep inspiration breath-hold technique for left-sided breast cancer: An analysis of predictors for organ-at-risk sparing. *Med. Dosim.* **40**, 89–95 (2015).
21. Taylor, C. W. *et al.* Estimating cardiac exposure from breast cancer radiotherapy in clinical practice. *Int. J. Radiat. Oncol. Biol. Phys.* **73**, 1061–1068 (2009).
22. Borger, J. H. *et al.* Cardiotoxic effects of tangential breast irradiation in early breast cancer patients: The role of irradiated heart volume. *Int. J. Radiat. Oncol. Biol. Phys.* **69**, 1131–1138 (2007).
23. Lorenzen, E. L., Brink, C., Taylor, C. W., Darby, S. C. & Ewertz, M. Uncertainties in estimating heart doses from 2D-tangential breast cancer radiotherapy. *Radiother. Oncol.* **119**, 71–76 (2016).
24. Ueda, Y., Gerber, N. K. & Das, I. J. Model-based cardiac dose estimation in radiation treatment of left breast cancer. *Br. J. Radiol.* **91**, 20180287 (2018).
25. Hiatt, J. R. *et al.* Dose-modeling study to compare external beam techniques from protocol NSABP B-39/RTOG 0413 for patients with highly unfavorable cardiac anatomy. *Int. J. Radiat. Oncol. Biol. Phys.* **65**, 1368–1374 (2006).
26. Koide, Y. *et al.* Synthetic breath-hold CT generation from free-breathing CT: A novel deep learning approach to predict cardiac dose reduction in deep-inspiration breath-hold radiotherapy. *J. Radiat. Res.* <https://doi.org/10.1093/jrr/rwab075> (2021).
27. Bakx, N. *et al.* Development and evaluation of radiotherapy deep learning dose prediction models for breast cancer. *Phys. Imaging Radiat. Oncol.* **17**, 65–70 (2021).
28. Hjelstuen, M. H. B., Mjaaland, I., Vikström, J., Madebo, T. & Dybvik, K. I. Pulmonary function tests—An easy selection method for respiratory-gated radiotherapy in patients with left-sided breast cancer. *Acta Oncol.* **54**, 1025–1031 (2015).
29. Lee, D., Dinniwel, R. & Lee, G. A retrospective analysis of lung volume and cardiac dose in left-sided whole breast radiotherapy. *J. Med. Imaging Radiat. Sci.* **47**, S10–S14 (2016).
30. Yamauchi, R., Mizuno, N., Itazawa, T., Saitoh, H. & Kawamori, J. Dosimetric evaluation of deep inspiration breath hold for left-sided breast cancer: Analysis of patient-specific parameters related to heart dose reduction. *J. Radiat. Res.* **61**, 447–456 (2020).
31. Mkanna, A. *et al.* Predictors of cardiac sparing in deep inspiration breath-hold for patients with left sided breast cancer. *Front. Oncol.* **8**, 1–6 (2018).
32. Czeremczyńska, B., Drozda, S., Górzynski, M. & Kępk, L. Selection of patients with left breast cancer for deep-inspiration breath-hold radiotherapy technique: Results of a prospective study. *Rep. Pract. Oncol. Radiother.* **22**, 341–348 (2017).
33. Browne, P. *et al.* Identifying breast cancer patients who gain the most dosimetric benefit from deep inspiration breath hold radiotherapy. *J. Med. Radiat. Sci.* **67**, 294–301 (2020).
34. Koide, Y. *et al.* Preoperative spirometry and BMI in deep inspiration breath-hold radiotherapy: The early detection of cardiac and lung dose predictors without radiation exposure. *Radiat. Oncol.* <https://doi.org/10.1186/s13014-022-02002-9> (2022).
35. Siddique, S. & Chow, J. C. L. Artificial intelligence in radiotherapy. *Rep. Pract. Oncol. Radiother.* **25**, 656–666 (2020).
36. Ronneberger, O., Fischer, P. & Brox, T. *U-Net: Convolutional Networks for Biomedical Image Segmentation. Medical Image Computing and Computer-Assisted Intervention—MICCAI 2015* 234–241 (Springer, 2015).
37. Zhang, R. *et al.* Diagnosis of coronavirus disease 2019 pneumonia by using chest radiography: Value of artificial intelligence. *Radiology* **298**, E88–E97 (2021).
38. Zargari Khuzani, A., Heidari, M. & Shariati, S. A. COVID-classifier: An automated machine learning model to assist in the diagnosis of COVID-19 infection in chest X-ray images. *Sci. Rep.* **11**, 9887 (2021).
39. Offersen, B. V. *et al.* ESTRO consensus guideline on target volume delineation for elective radiation therapy of early stage breast cancer. *Radiother. Oncol.* **114**, 3–10 (2015).
40. Feng, M. *et al.* Development and validation of a heart atlas to study cardiac exposure to radiation following treatment for breast cancer. *Int. J. Radiat. Oncol. Biol. Phys.* **79**, 10–18 (2011).
41. Moons, K. G. M. *et al.* Transparent reporting of a multivariable prediction model for individual prognosis or diagnosis (TRIPOD): Explanation and elaboration. *Ann. Intern. Med.* **162**, W1–W73 (2015).
42. Schroeder, J. D. *et al.* Prediction of obstructive lung disease from chest tomographs via deep learning trained on pulmonary function data. *Int. J. Chron. Obstruct. Pulmon Dis.* **15**, 3455–3466 (2020).
43. Bloomfield, D. J. Core Group facilitated by The Royal College of Radiologists. Development of Postoperative Radiotherapy for Breast Cancer: UK consensus statements—A model of patient, clinical and commissioner engagement? *Clin. Oncol.* **29**, 639–641 (2017).
44. Locke, I. & Drinkwater, K. Implementation of Royal College of Radiologists Consensus Statements and National Institute for Health and Care Excellence Guidance: Breast radiotherapy practice in the UK. *Clin. Oncol.* **33**, 419–426 (2021).

45. Kavousi, M. *et al.* Evaluation of newer risk markers for coronary heart disease risk classification: A cohort study. *Ann. Intern. Med.* **156**, 438–444 (2012).
46. Mast, M. E. *et al.* Less increase of CT-based calcium scores of the coronary arteries. *Strahlenther. Onkol.* **192**, 696–704 (2016).
47. Lloyd-Jones, D. M. *et al.* Framingham risk score and prediction of lifetime risk for coronary heart disease. *Am. J. Cardiol.* **94**, 20–24 (2004).

Acknowledgements

The authors thank all the patients, investigators, and institutions involved in this study.

Author contributions

T.A., H.S., T.Ki. and R.M. collected the data. H.T., and T.Ko. interpreted the data and supervised the study. All authors reviewed and approved the final manuscript.

Funding

This work was supported by Aichi Cancer Research Foundation, Hori Sciences and Arts Foundation, and JSPS KAKENHI Grant-in-Aid for Early-Career Scientists (Grant Number 20K16402).

Competing interests

The authors declare no competing interests.

Additional information

Correspondence and requests for materials should be addressed to Y.K.

Reprints and permissions information is available at www.nature.com/reprints.

Publisher's note Springer Nature remains neutral with regard to jurisdictional claims in published maps and institutional affiliations.



Open Access This article is licensed under a Creative Commons Attribution 4.0 International License, which permits use, sharing, adaptation, distribution and reproduction in any medium or format, as long as you give appropriate credit to the original author(s) and the source, provide a link to the Creative Commons licence, and indicate if changes were made. The images or other third party material in this article are included in the article's Creative Commons licence, unless indicated otherwise in a credit line to the material. If material is not included in the article's Creative Commons licence and your intended use is not permitted by statutory regulation or exceeds the permitted use, you will need to obtain permission directly from the copyright holder. To view a copy of this licence, visit <http://creativecommons.org/licenses/by/4.0/>.

© The Author(s) 2022